Membrane cholesterol extraction decreases Na+ transport in A6 renal epithelia
Peer-reviewed author version

BALUT, Corina; STEELS, Paul; RADU, Mihai; AMELOOT, Marcel; VAN
DRIESSCHE, Willy & JANS, Danny (2006) Membrane cholesterol extraction
decreases Na+ transport in A6 renal epithelia. In: AMERICAN JOURNAL OF
PHYSIOLOGY-CELL PHYSIOLOGY, 290(1). p. C87-C94.

Membrane Cholesterol Extraction decreases Na$^+$ Transport in A6 Renal Epithelia

by

Corina Balut[1,3], Paul Steels[1], Mihai Radu[1,4], Marcel Ameloot[1], Willy Van Driessche[2], and Danny Jans[1]

(1) Hasselt University
Laboratory of Physiology
Agoralaan 1 D
B-3590 Diepenbeek, Belgium

(2) K. U. Leuven
Laboratory of Physiology
Campus Gasthuisberg
B -3000 Leuven, Belgium

Running title: Renal Electrolyte Transport and Membrane Cholesterol Content

Address correspondence to:

Danny Jans

Tel. 0032-11-26.85.23

Fax 0032-11-26.85.99

Email: danny.jans@uhasselt.be

ABSTRACT

In this study we investigated the dependence of Na^+ transport regulation on membrane cholesterol content in A6 epithelia. We continuously monitored the short-circuit current (I_{SC}), the transepithelial conductance (G_T) and the transepithelial capacitance (C_T) to evaluate the effects of cholesterol extraction from the apical and basolateral membranes in steady-state conditions and during activation with a hypo-osmotic shock, oxytocin and adenosine. Cholesterol extraction was achieved by perfusing the epithelia with methyl-β-cyclodextrin (mβCD) for 1h. In steady-state conditions, apical membrane cholesterol extraction did not significantly affect the electrophysiological parameters, in contrast to the marked reductions observed during basolateral mβCD treatment. However, apical mβCD application hampered the responses of I_{SC} and G_T to hypotonicity, oxytocin and adenosine. Analysis of the blocker-induced fluctuation in current demonstrated that apical mβCD treatment decreased the epithelial sodium channel open probability in steady-state as well as after activation of Na^+ transport by adenosine, whereas the density of conducting channels was not significantly changed, as confirmed by C_T measurements. Na^+ transport activation by hypotonicity was abolished during basolateral mβCD treatment due to a reduced Na^+/K^+ pump activity. From this study we conclude that basolateral membrane cholesterol extraction reduces Na^+/K^+ pump activity, whereas the reduced cholesterol content of the apical membranes affects the activation of Na^+ transport by reducing the sodium channel open probability.

INTRODUCTION

Cholesterol is a prominent component of mammalian plasma membranes and an important factor in determining membrane functions (26). Within the cell membrane cholesterol plays an active role, regulating the lipid bilayer dynamics and structure by modulating the packing of phospholipid molecules (18). Recent studies suggest that cholesterol is involved in the assembly and maintenance of sphingolipid-cholesterol rich microdomains, called rafts, proposed to act as platforms that have functional implications in signal transduction, intracellular trafficking of lipids and proteins and in translocation of solutes across the membrane (5, 12, 27). It was proposed that cholesterol modulates the activity of various membrane transporters, e.g., the Ca^{2+} channel (3), the Na/P_i cotransporter from renal cells (31) or the Ca^{2+}-ATPase (21) and Na^+/K^+-ATPase in a variety of cells including erythrocytes, endothelial or renal epithelial cells (17, 21, 32).

To date, there is little evidence for abnormal regulation of the epithelial sodium channel (ENaC) – mediated Na^+ transport in renal epithelial cells induced by changes in the cholesterol content of the cell membrane bilayer. Acting at the apical membrane, ENaC activity is modulated to fine-tune Na^+ reabsorption in a number of tight epithelia and maintain body salt and fluid balance (24). Data obtained on A6 epithelia show that endogenously-expressed Na^+ channels are associated with rafts, both intracellularly and on the cell surface (11). Heterologously-expressed ENaC has also been described as being incorporated in rafts in COS7 and HEK293 cells (23). At the same time, reconstitution of functional amiloride-sensitive Na^+ channels obtained from A6 cultured renal epithelial cells into artificial planar lipid bilayer membranes show that ENaC is restricted to detergent-resistant membrane microdomains and that preservation of native protein-lipid interactions is important for the biological activity of extracted channels (25). On the other hand, it has been shown that lipid-modifying agents do not affect Na^+ transport in steady-state conditions (25). A recent study addresses the issue of ENaC regulation by the changes in membrane lipid order induced by temperature or chemical compounds (2).

In this study, we investigate the effects of a reduced membrane cholesterol environment on Na^+ transport in A6 epithelia. We compare with electrophysiological

tools (continuous recording of short-circuit current (I_{SC}), transepithelial conductance (G_T), transepithelial capacitance (C_T) and by blocker-induced noise analysis) ion transport before and after membrane cholesterol depletion on either apical or basolateral side in steady-state conditions and in response to three stimuli that involve different mechanisms and pathways of activation: (1) a hypotonic shock activates Na^+ transport in A6 epithelia through pathways that depend on an extracellular Ca^{2+}-sensitive mechanism, presumably a Ca^{2+}-sensing receptor in the basolateral membrane (15); (2) oxytocin uses the cAMP pathway, that enhances Na^+ transport via ENaC insertion; (3) adenosine, when applied to the basolateral side, restricts to the activation of Na^+ transport alone, while it does not affect transepithelial Cl^- transport, which is not the case for both other activators.

Our results show that cholesterol extraction from the apical membranes affects Na^+ transport activation by reducing sodium channel open probability without affecting sodium channel insertion. In contrast, basolateral membrane cholesterol extraction abolishes steady-state Na^+ transport and its activation by reducing Na^+/K^+ pump activity.

METHODS

Cell culture

A6 cells (obtained from Dr. J. P. Johnson, University of Pittsburgh, Pittsburgh, PA) were cultured to confluence at 28 °C in an atmosphere of humidified air, supplemented with 1% CO_2. The cells were fed twice weekly with growing medium consisting of a 1:1 mixture of Leibovitz's L-15 and Ham's F-12 media, supplemented with 10 % fetal bovine serum (Sigma, St Louis, MO, USA), 2.6 mM sodium bicarbonate, 3.8 mM L-glutamine, 95 $IU.ml^{-1}$ penicillin, and 95 $mg.ml^{-1}$ streptomycin. All experiments were carried out at room temperature on cell passages 86 – 97 and 107. For electrophysiological measurements, cells were allowed to form polarized monolayers on permeable inorganic membranes (Anopore, pore size 0.2 mm; Nunc Intermed, Roskilde, Denmark). Electrophysiological and volume measurements were performed on similar monolayers cultured between 23 and 30 days after seeding the cells.

Cholesterol depletion procedure

Membrane cholesterol depletion was accomplished under continuous measurement conditions by perfusing the apical/basolateral side of monolayers for 60 min with indicated saline solution containing either 10 or 20 mM methyl-β-cyclodextrin (mβCD). Due to its high affinity for sterols, as compared to other lipids, mβCD has been used extensively in recent years as an effective tool for manipulating the cell membrane cholesterol level both '*in vitro*' and '*in vivo*' (6, 11, 22). Distinct Na^+ reabsorption stimulating procedures (hypo-osmotic shock and treatment with oxytocin and adenosine) were applied and performed in the absence and presence of the mβCD solution.

Electrophysiological measurements

To perform the electrophysiological measurements, membranes supporting the confluent cell layer were mounted in an Ussing-type chamber (7) and short-circuited with a high-speed voltage clamp. The equipment and theoretical background for electrophysiological and impedance measurements have been extensively described previously (29).

Noise analysis

The pulse protocol method of blocker-induced noise analysis was used to determine the effect of apical cholesterol extraction on single channel current (i_{Na}), channel open probability (P_O) and functional channel density (N_T) of the amiloride-sensitive Na$^+$ channel during steady state and adenosine activated Na$^+$ transport. Noise analysis was implemented by using a reversible blocker of the apical Na$^+$ channel, 6-chloro-3,5-diaminopyrazine-2-carboxamide (CDPC), following the theory and protocols described previously (4). The blocker on-(k_{on}) and off-(k_{off}) rates were calculated by linear regression analysis of the corner frequency values (f_c) recorded at different CDPC concentrations, following a stepwise increase protocol.

Current noise power density spectra were recorded while switching every 5 min the apical CDPC concentration between 10 and 40 μM. Three pulses were applied in each considered state: control, treatment with mβCD and response to adenosine. CDPC-induced noise measurements were performed for mβCD exposed cells during the last 30 minutes of the 1 h treatment. In adenosine-stimulated cells, the noise measurements were started in the highly activated Na$^+$ transport conditions, 30 min after the initiation of the agonist.

Cell volume measurements

Cell volume changes were monitored by measuring cell thickness (T_c), as published before (28). T_c is expressed as percentage relative to the value recorded just before imposing the hypo-osmotic challenge. Averaged values of T_c were calculated from the recordings corresponding to the beads that remained attached to the monolayer during the entire experiment. N represents the number of measured tissues and n is the number of beads used to calculate the average.

Membrane permeabilization

Nystatin, at a concentration of 50 I.U./ml, was used to permeabilize the apical membranes with the aim to further characterize the changes induced by basolateral cholesterol extraction on Na$^+$/K$^+$-ATPase activity (20). Progression of the apical permeabilization was evaluated by impedance measurements, while simultaneously recording I_{SC} and G_T to monitor changes in the basolateral membrane transport activity.

Solutions and chemicals

Table 1 summarizes the composition of the solutions used for electrophysiological and volume measurements. In this study we used isosmotic (260 mosmol/kg H_2O), hyposmotic (140 mosmol/kg H_2O) and solutions of 200 mosmol/kg H_2O, at pH = 8.2. Experiments with solutions at 200 mOsm/kg H_2O were bilaterally equi-osmolal.

To extract cholesterol from the apical/basolateral membranes we have used solutions containing 20 mM mβCD in all our experiments, except for evaluation of ENaC kinetics in response to adenosine. Due to the fact that this protocol does not allow recirculation of the perfusing solutions, for these experiments, cells were treated with 10 mM mβCD to avoid chemicals waste and reduce the cost of the experiments. Methyl-beta-cyclodextrin (mβCD) at a concentration of 20 mM substantially contributes to the final osmolality of the working solution. Therefore, the mβCD containing solutions at different osmolalities were prepared by taking into account this contribution. The osmolality of the control solutions was adjusted with sucrose while maintaining the same Na^+ concentration as in the corresponding mβCD experiments (Table 1). Methyl-beta-cyclodextrin at 10 mM was simply added to the perfusing solution. During stimulating procedures, the concentrations of Na^+ on apical and basolateral side were equal, in order to avoid a gradient for this ion across the epithelium, and transepithelial currents through the paracellular pathway.

Oxytocin (Oxy) and adenosine were added basolaterally, at a concentration of 0.1 I.U./ml and 1 μM, respectively. Amiloride (Ami, 0.1 mM) was added to the apical bath to determine the amiloride-insensitive component of I_{SC}. CDPC (stock solution in dimethyl sulfoxide) was used in concentrations up to 200 μM.

Most substances were purchased from Merck, except amiloride, oxytocin, and adenosine (Sigma), CDPC (Aldrich) and mβCD (Fluka).

Data analysis

Results are given as means $\pm$ standard error (S.E.M.) along with the number (N) of epithelia investigated. All comparisons between the control and experimental groups were done by Student's t-test, and statistical significance was defined as $P < 0.05$.

RESULTS

Apical mβCD treatment depresses Na$^+$ transport activation in response to a hypotonic shock

Initially, tissues were exposed to a hypo-osmotic solution (140 mosmol/kg H$_2$O) on the apical side and to an iso-osmotic solution (260 mosmol/kg H$_2$O) on the basolateral side and allowed to stabilize to a steady-state level that was maintained for at least 30 minutes. Control cells were kept as such for an extra period of 60 min and were subsequently subjected to a hypo-osmotic shock by the sudden reduction of the basolateral solution osmolality to 140 mosmol/kg H$_2$O. In parallel experiments, prior to the hypo-osmotic challenge, A6 epithelia were exposed at the apical side to a solution containing 20 mM mβCD for 60 minutes. Next, the hypo-osmotic shock was applied in the presence of apical mβCD for this set of tissues.

As described previously (29), after a fast but transient decrease of C_T visible within 30 s of hypotonicity, C_T exhibits a slow biphasic increase reaching a maximum after 18 min of hypotonicity. Likewise, both I_{SC} and G_T show a biphasic, synchronous rise but require ~60 min of hypotonicity to reach a plateau. Figure 1 shows comparatively the changes of I_{SC}, G_T and C_T in control and apically mβCD-treated tissues as a response to the hypotonic challenge. The corresponding mean values obtained in basal level and at the end of the hypotonic period for each case are summarized in Table 2 – S1. The rise in I_{SC} and G_T mainly reflects transepithelial Na$^+$ absorption. This is demonstrated by adding 0.1 mM amiloride to the apical bath at the end of the hypo-osmotic shock, causing a sudden drop in I_{SC} and G_T close to the starting values.

The presence of mβCD in the apical compartment does not significantly affect the electrical behavior of A6 epithelia during steady-state conditions. After 60 min of perfusion with the mβCD solution, I_{SC} merely changed from 0.8 ± 0.1 to 1.1 ± 0.2 μA/cm^2, G_T remained constant at 0.07 ± 0.01 mS/cm^2, while C_T barely changed from 0.80 ± 0.01 to 0.81 ± 0.01 μF/cm^2 (N=5, P>0.05). However, apical mβCD treatment significantly impaired the activation of I_{SC} and G_T in response to hypotonicity (Fig. 1, Table 2): the I_{SC} increase was inhibited with 40% (P=0.001), while G_T was 43% less stimulated (P=0.008) as compared to control cells. Interestingly, the increase in C_T for cholesterol depleted cells was not significantly different from the control tissues: 73 ±

7 % as compared to 66 $\pm$ 4 %, respectively (P > 0.05). In addition, mβCD treatment activated a transient (2~3 min) apical conductance during hypo-osmotic conditions: in mβCD-treated cells, immediately after imposing the hypotonic shock, I_{SC} increased rapidly with 1.6 $\pm$ 0.3 μA/cm^2, while G_T temporarily increased with 0.09 $\pm$ 0.02 mS/cm^2 (Fig. 1). This phenomenon, absent after basolateral substitution of Cl$^-$ for SO_4^{2-} reflects a transient Cl$^-$ secretion.

Apical mβCD treatment depresses the oxytocin response

In this set of experiments tissues were allowed to stabilize in solutions of slightly reduced osmolality (200 mosmol/kg H$_2$O) in order to elevate the basal level of Na$^+$ transport. Even though, in 200 mosmol/kg H$_2$O solutions, apical cholesterol depletion did not significantly affect the basal electrical parameters. I_{SC} presented a variation from 15.8 $\pm$ 0.7 to 15.6 $\pm$ 0.7 μA/cm^2, while G_T changed from 0.19 $\pm$ 0.01 to 0.18 $\pm$ 0.01 mS/cm^2 (N=4). C_T increased slightly, but not significantly, from 0.72 $\pm$ 0.02 to 0.74 $\pm$ 0.02 μF/cm^2 (P > 0.05). However, with oxytocin at the basolateral side, Na$^+$ transport activation for apically mβCD-treated cells was likely depressed as during the hypotonic response (Table 2 – S2): 45% inhibition for the I_{sc} increase (P < 0.001) and 30% less stimulation of G_T (P = 0.003) as compared to control cells. It is important to notice that the C_T values did not significantly differ between cholesterol depleted and control tissues (P > 0.05).

Effects of acute apical mβCD treatment on elevated levels of Na$^+$ transport

So far, apical cholesterol extraction apparently does not affect basal Na$^+$ transport in isosmotic, as well as in media of 200 mosmol/kg H$_2$O. It is conceivable that mβCD might exerts a significant effect at elevated levels of Na$^+$ transport. Therefore, we performed experiments in which we monitored the effect of mβCD after maximal stimulation of Na$^+$ transport, induced by exposing the epithelia to an hyposmotic shock. The mβCD treatment was administered after I_{SC} almost reached its maximal value, 40 min after the initiation of the hypotonic challenge. Figure 2 displays similar time courses of I_{SC}, G_T and C_T for this approach in control and apically mβCD-treated cells for the first 30 min after mβCD application. Next, the control cells stabilized on a plateau level, whereas a slight decrease could be observed in the presence of mβCD. However, statistical analysis did not indicate a significant difference between

mβCD-subjected cells and control cells for the indicated period. At the end of the cholesterol depletion treatment period, I_{SC} measured 6.2 ± 0.4 μA/cm^2 as compared to the control 7.0 ± 0.5 μA/cm^2 (N=5). G_T reached 0.11 ± 0.01 mS/cm^2 in treated cells as compared to 0.12 ± 0.01 mS/cm^2 in control, whereas C_T measured 0.95 ± 0.06 μF/cm^2 in treated cells as compared to 0.98 ± 0.06 μF/cm^2 in control (P > 0.05).

Effects of apical cholesterol extraction in response to adenosine - Evaluation of ENaC kinetics

The results obtained so far indicate that the presence of mβCD in the apical bath depressed sodium transport activation without affecting the increase in C_T. Because C_T is proportional to the area of the apical membrane, it appears as if the treatment with mβCD does not affect membrane trafficking. Therefore, we intended to monitor the changes of Na$^+$ channel density during Na$^+$ transport activation and the effect of mβCD on this parameter. If a correlation between membrane area and Na$^+$ channel density is also maintained in these experiments, the reduction of Na$^+$ transport activation is presumably caused by effects on the individual channel, i.e., single channel current or open channel probability.

First, we investigated the effects of 10 mM mβCD on I_{SC}, G_T and C_T in steady-state conditions and in response to adenosine. Figure 3 illustrates the time profiles for I_{SC}, G_T and C_T in response to adenosine in control cells and mβCD-treated ones. Apical mβCD treatment did not significantly affect the basal, steady-state values of the monitored parameters. During the treatment, I_{SC} changed from 11.6 ± 0.9 to 12.9 ± 0.4 μA/cm^2, G_T from 0.15 ± 0.01 to 0.16 ± 0.01 mS/cm^2 and C_T from 0.71 ± 0.01 to 0.73 ± 0.01 μF/cm^2 (N=5, P > 0.05). It is important to note that 10 mM mβCD reduced the activation of Na$^+$ transport in response to basolateral adenosine to a similar level as reported above with 20 mM mβCD during the hypotonic shock and with oxytocin stimulation. The mean values obtained for I_{SC}, G_T and C_T in basal level and in response to adenosine stimulation for control and apically mβCD-perfused cells are listed in Table 2-S3. Thus, for the mβCD-treated cells I_{SC} stimulation in response to adenosine was inhibited with 47% (P = 0.002) and G_T with 50% (P=0.002). Again, in these experiments the maximum increase in C_T was not significantly different for both types of tissues, increasing with about 10% in both cases.

Noise analysis parameters: blocker rate coefficients and i_{Na}, P_o and N_T in relation to apical cholesterol extraction

Noise analysis was used to determine the contribution of i_{Na}, P_o and N_T to the measured I_{sc} in steady-state conditions and in response to adenosine, for control and apically cholesterol extracted cells. Figure 4A illustrates the linear relationship between $2\pi f_c$ (equal to the chemical rate of the current-modulating process) and the CDPC concentration in the absence (control) and in the presence of 10 mM mβCD in the apical solution (the values are calculated as an average from 6 recordings). The *ON* and *OFF* rates for CDPC during control periods were consistent with those previously reported (14): $2\pi f_c = 7.78\ [CDPC]_{ap} + 252.9$. However, mβCD reduced the k_{on} rate, but did not affect the k_{off} rate (P>0.05): $2\pi f_c = 1.94\ [CDPC]_{ap} + 264.8$. The results for i_{Na}, N_T and P_o in control conditions (basal level and response to adenosine stimulation) and after 1h apical treatment with 10 mM mβCD are presented as bar diagrams (Fig. 4B). For control cells, adenosine increased N_T from 102 ± 6 to $217 \pm 22\ \mu m^{-2}$ (N=4, P<0.05). P_o slightly decreased in the presence of adenosine from 0.46 ± 0.02 to 0.36 ± 0.05, while i_{Na} merely changed during the stimulation from 0.32 ± 0.02 to 0.30 ± 0.02 pA (P>0.05). During mβCD treatment N_T changed from 104 ± 7 to $129 \pm 12\ \mu m^{-2}$ (N=4, P > 0.05), while P_o decreased significantly from 0.44 ± 0.01 to 0.28 ± 0.04 (P<0.05), and i_{Na} slightly increased from 0.32 ± 0.01 to 0.37 ± 0.01 pA (P<0.05). Even though P_o decreased after cholesterol extraction, the I_{SC} values do not significantly change during 60 min exposure to mβCD, due to the increase in N_T and i_{Na}. In the presence of mβCD, adenosine increased N_T to $239 \pm 38\ \mu m^{-2}$ (N=4, P<0.05), slightly decreased P_o to 0.21 ± 0.04 (P>0.05), and reduced i_{Na} to 0.33 ± 0.02 pA (P>0.05). Based on these values, the calculated I_{SC} in response to adenosine was less elevated after treatment with mβCD as compared to control cells, as confirmed by the I_{sc} recordings. An important finding is that the N_T increase in response to adenosine is similar for the cholesterol-extracted cells as for the control cells. This result is in agreement with the C_T measurements, indicating that the main effect of lowering membrane cholesterol is reflected in the ENaC activity (P_o) and not in the channel trafficking processes at the apical membrane.

Effects of basolateral treatment with mβCD on I_{SC}, G_T and C_T in steady state level and in response to hypo-osmotic shock - Volume regulation after basolateral cholesterol extraction

After stabilization period, cells were basolaterally perfused with 20 mM mβCD for a period of 60 min. Next, the hypo-osmotic challenge was induced by decreasing the osmolality of the basolateral solution to 140 mosmol/kg H_2O, while keeping mβCD in the hypo-osmotic perfusate. Figure 5 illustrates how lowering cholesterol at the basolateral side affects the time courses of I_{SC}, G_T and C_T. The typical time course for these parameters in control experiment was shown in figure 1. During mβCD treatment I_{SC} significantly decreased from 1.7 ± 0.3 to 0.7 ± 0.2 µA/cm^2 (N=4, P < 0.05). Moreover, the stimulation of Na$^+$ transport in response to hypotonicity was completely abolished. After 60 min of hypotonicity, I_{SC} merely increased with 1.9 ± 0.3 µA/cm^2, relative to the starting value. During the cholesterol extraction, G_T increased slowly from 0.10 ± 0.02 to 0.15 ± 0.02 mS/cm^2. At the end of the hypotonic challenge, G_T levels increased dramatically. Basolateral mβCD treatment did not change C_T significantly, which slowly increased from 0.81 ± 0.02 to 0.85 ± 0.03 µF/cm^2 (P > 0.05). However, a more striking effect could be observed in C_T during the hypotonic stress. C_T enhanced only with 25.3 ± 2.3 % from the starting value 0.90 ± 0.05 µF/cm^2, as compared to the control cells, which increased with 65.5 ± 2.3 % from the basal value of 0.90 ± 0.05 µF/cm^2.

Given the remarkable effects observed in the electrical parameters during the hypotonic stimulation when mβCD was applied at the basolateral border, we next tested whether cholesterol depletion at the basolateral side affected the regulatory volume decrease (RVD) during hypotonic stress. Interestingly, after 60 minutes of mβCD treatment, cells maintained a normal RVD: epithelial cell thickness, T_c, increased in response to cell swelling with 50.8 ± 3.2 % (N=4, n=44) in treated cells as compared to control tissues 48.8 ±1.6 % (N=4, n=41). In both cases cells regulated their volume back within 30 min, while being continuously exposed to the hypo-osmotic solutions.

Basolateral cholesterol depletion affects the activity of the Na^+/K^+ pump

To explore a possible involvement of the Na^+/K^+ pump in the I_{SC} drop and the lack of response of the basolateral mβCD-treated cells to the hypotonic stimulation, we permeabilized the apical membrane with nystatin. This manoeuvre allows electrical uncoupling of the two membrane areas of the epithelium to evaluate the transport processes that take place at the basolateral membrane (19, 20).

For this set of experiments, cells were allowed to stabilize in identical iso-osmotic solutions on both sides. Introducing 50 I.U./ml nystatin in the apical bath increased the apical Na^+ conductance and, as a consequence, the elevated level of cytosolic Na^+ highly activates the extrusion process across the basolateral membrane by the Na^+/K^+ pump (19). Apical membrane permeabilization was assessed by impedance measurements. Nyquist plots showed transition from the unpermeabilized state, a single impedance locus, to the permeabilized apical membrane, appearance of two loci in the impedance spectra. Typical time courses of G_T and I_{SC} in response to nystatin action are depicted in figure 6. I_{SC} rapidly increased after addition of nystatin from the basal level 0.5 ± 0.1 to 6.5 ± 0.6 μA/cm^2, reaching a maximum within 5 min and maintaining it for at least 20 min. This increase has been demonstrated in previous studies to be related to active cation transport in epithelia by the basolateral Na^+/K^+-ATPase (8). The G_T increase, related to the reduction of the apical membrane resistance under the nystatin treatment, ranged from 0.36 ± 0.04 to 0.66 ± 0.06 mS/cm^2 and remained constant for the same period of time.

After 20 minutes of stable high rate activity of the Na^+/K^+-pump, cholesterol extraction was initiated by perfusing the basolateral side of the cells with a solution containing 20 mM mβCD for 1 h, while nystatin was kept in the apical perfusion solution. Treatment with mβCD induced a small transient increase in I_{SC} followed by a continuous decrease, indicating alterations at the level of Na^+/K^+-pump activity, while G_T presented a continuous slow increase for the first 40 minutes of cholesterol extraction followed by a more sharp increase within the last 20 minutes of treatment, towards values indicating tissue damage.

DISCUSSION

In this paper, we analyzed the role of a reduced membrane cholesterol environment in regulating electrogenic ion transport in renal A6 epithelial cells. We extracted cholesterol from either the apical or the basolateral membranes from the A6 cells. Removal of membrane cholesterol was ensured by exposing the cells to mβCD, a water-soluble cyclic carbohydrate with high specificity for sterols. During cholesterol extraction electrophysiological parameters were monitored continuously in two conditions: (a) stationary conditions, i.e., at different steady-state levels of Na^+ channel activation; and (b) in response to three types of stimulating procedures: a hypotonic shock, and basolateral application of either oxytocin or adenosine. The main findings reported in our study are: (1a) cholesterol depletion of the apical membranes does not affect the steady-state levels of Na^+ transport; but (1b) impairs Na^+ transport activation in response to all stimulating procedures by decreasing ENaC open probability without affecting channel insertion; (2a) cholesterol depletion of the basolateral membranes strongly affects basal levels of Na^+ transport; and (2b) blocks Na^+ transport activation by impairing the activity of the Na^+/K^+-ATPase without disturbing cell volume regulation.

(1) cholesterol depletion and steady-state levels of Na^+ transport

Constitutive levels of Na^+ transport are apparently not dependent on the level of cholesterol in the apical membranes. This finding is in agreement with other studies reporting that agents known to modify the amount of lipids (cholesterol and sphingolipids) in cell membranes do not affect the amiloride-sensitive transepithelial current (25). However, when analyzing the current constituents by noise analysis, we observed a significant decrease in ENaC open probability after apical mβCD treatment. Noise analysis data suggest that the same level of macroscopic short-circuit current is maintained by a rise in channel density. The decrease in the number of active channels is a possible consequence of the change in protein conformation. A potential cause is the distortion of hydrophobic interactions in the phospholipids bilayer after altering the physical properties of the membrane lipid environment. Such a concept is supported by the observation that cholesterol removal leads to an increase in membrane fluidity (10) and to a decrease in lipid order (9). The difference in perceptivity between apical and basolateral membranes

to mβCD treatment may be due to a dissimilarity in architecture between both borders. The apical side, exposed to the outside, is covered by an intricate structure of glycolysated proteins and lipids for protection, whereas the basolateral sides need to be more open, yet more vulnerable.

(2) apical cholesterol depletion impairs Na$^+$ transport stimulation by lowering ENaC open probability

Independent of the pathway that leads to Na$^+$ transport activation in A6 epithelia, all stimuli used in this study are less effective in doing their job after apical cholesterol depletion. In addition, noise analysis data indicated a decrease in ENaC open probability as the main cause for this impediment. Interestingly, the observed decrease in I_{sc} and G_T stimulation is not paralleled by a diminished increase in C_T. The absence of a difference in C_T changes between control cells and apically cholesterol-extracted cells indicates that, no matter what the underlying mechanism of activation is, whether it is an increased insertion or a decreased retrieval of ENaC proteins, it is independent of the cholesterol level of the apical membranes. This hypothesis is supported by the noise analysis data showing that the increase in total channel density (N_T) is in the same range between control and apically cholesterol-depleted cells.

The observation of the reduced open probability for the amiloride-sensitive channels in the presence of mβCD depends on correct interpretation of the data obtained from the current fluctuation measurements (30). These data show that in the presence of mβCD, CDPC is less effective in blocking ENaC. This is demonstrated by the decrease in the *ON* rate constant of the blocker. Such an effect is most likely caused by a direct interaction between the cholesterol-depleting drug and the blocker. Alternatively, a competition between the two compounds for binding to the channel can be considered. A direct binding between mβCD and ENaC is unlikely to occur. Such a mechanism would lower ENaC activity instantaneously, whereas effects on ENaC behavior in the presence of mβCD only become apparent at least 30 min after perfusion with the cholesterol-depleting drug.

(3) basolateral cholesterol depletion impairs Na$^+$ transport stimulation by attenuating the Na$^+$,K$^+$-ATPase activity

Basolateral cholesterol extraction induces more rapid and dramatic changes in the electrical parameters of the epithelium. Both steady-state and hyposmotic-activated levels of Na^+ reabsorption are inhibited by basolateral mβCD treatment. Na^+ transport across the epithelium requires the concerted activity of both basolateral K^+ channels and the Na^+/K^+-ATPases. Two observations support the idea that the presence of mβCD at the basolateral border affects the activity of the pump. To properly evaluate the transport processes that take place at the basolateral border, independent of ENaC activity in the apical membrane, we electrically uncoupled the two cell membranes by permeabilizing the apical membrane with nystatin. Such an approach increases Na^+ delivery to the pump nearby the saturating level, making the observed short-circuit current an index of the Na^+/K^+-ATPase activity. The observed decrease of the I_{SC} during basolateral mβCD treatment is therefore a reliable indication of the lowered activity of the pump. These results are supported by other studies that show that normal functioning of the Na^+/K^+-ATPase depends on the membrane cholesterol content in a variety of cell types, including renal cells (32). Effects of basolateral mβCD on basolateral K^+ channels is unlikely to be involved, given the ability of the epithelia to perform normal regulatory volume decrease in these conditions, a process that requires full activity of the basolateral K^+ channels, although not identical, at least similar in structure and thus probably having a comparable sensitivity to cholesterol depletion.

Basolateral cholesterol extraction also impairs the C_T rise during hypotonicity. The transient rise of C_T during hypotonicity reflects the changes in the intracellular free Ca^{2+} concentration ($[Ca^{2+}]_i$) that occur during the hypo-osmotic shock (14). It is conceivable that the reduced basolateral membrane cholesterol level affects one of the underlying mechanisms. Recently, it has been reported that activation of Na^+ transport by hypotonicity in the A6 epithelia can occur in the absence of $[Ca^{2+}]_i$ changes. Therefore, it is likely that the observed C_T changes are not related to the activation of I_{sc} during the hypo-osmotic conditions. The impaired C_T rise in response to the hypo-osmotic shock for basolateral mβCD-treated cells resembles the C_T rise that is observed when Mg^{2+} is included in the basolateral perfusion solutions (14). Basolateral Mg^{2+} blocks non-capacitative Ca^{2+} entry in A6 epithelia that occurs during osmotic adaptation of the cells (13). A similar behavior was observed in rat basophil

leukemia cells, in which mβCD significantly inhibited Ca^{2+} influx from the extracellular medium but did not affect Ca^{2+} release from intracellular Ca^{2+} stores (16).

In conclusion, by combining the above findings it can be expected that a reduced body cholesterol level, induced either by pharmaceuticals that block cholesterol synthesis, such as statins, or, by compounds that extract cholesterol from the membranes, for instance when cyclodextrins are used as vehicles for pharmaceutical delivery, body salt loss may occur as a consequence of impairing the activation of Na^+ reabsorption in the distal parts of the nephron by both reducing the number of open ENaC channels in the apical membranes and rendering the Na^+/K^+-ATPases in the basolateral membranes less effective. The fundamental question for understanding the mechanisms by which cholesterol affects the function of membrane proteins is whether cholesterol regulates protein function by specific sterol-protein interactions (direct binding to the protein of interest or to a modulatory protein) or by changing the physical properties of the lipid environment. As expected, cholesterol removal increases membrane fluidity (10) and decreases lipid order (9) but altering the level of cholesterol alone cannot discriminate between the two mechanisms, because both the amount of cholesterol and the physical properties of the membrane are altered at the same time. This issue requires further complex investigations. Understanding the mechanisms by which the lipid membrane environment participates in regulation of ion transport activation in epithelial cells, actively involved in salt reabsorption and body fluid control, may have broad implications in elucidating physiological and pathophysiological aspects of blood pressure regulation.

Acknowledgments

References

1. **Atia, F, Mountian I, Simaels J, Waelkens E, and Van Driessche W.** Stimulatory effects on Na$^+$ transport in renal epithelia induced by extracts of *Nigella arvensis* are caused by adenosine. *J Exp Biol* 205(Pt 23): 3729-3737, 2002.

2. **Awayda, MS, Shao W, Guo F, Zeidel M, and Hill WG.** ENaC-Membrane interactions: regulation of channel activity by membrane order. *J Gen Physiol* 123: 709-727, 2004.

3. **Bialecki, RA, and Tulenko TN.** Excess membrane cholesterol alters calcium channels in arterial smooth muscle. *Am J Physiol* 257: C306– C314, 1989.

4. **Blazer-Yost, BL, Liu X, and Helman SI.** Hormonal regulation of ENaCs: insulin and aldosterone. *Am J Physiol* 274: C1373-C1379, 1998.

5. **Brown, DA, and London E.** Functions of lipid rafts in biological membranes. *Annu Rev Cell Dev Biol* 14:111-136, 1998.

6. **Christian, AE, Haynes MP, Phillips MC, and Rothblat GH.** Use of cyclodextrins for manipulating cellular cholesterol content. *J Lipid Research* 38: 2264-2272, 1997.

7. **De Wolf, I and Van Driessche W.** Voltage-dependent Ba^{2+} block of K$^+$ channels in the apical membrane of frog skin. *Am J Physiol* 251: C696–C706, 1986.

8. **Fujii, Y, and Katz AI.** Direct Na$^+$-K$^+$ pump stimulation by K$^+$ in cortical collecting tubules: a mechanism for early renal K$^+$ adaptation. *Am J Physiol* 257: F595-F601, 1989.

9. **Gidwani, A, Holowka D, and Baird B.** Fluorescence anisotropy measurements of lipid order in plasma membranes and lipid rafts from RBL-2H3 mast cells. *Biochemistry* 40: 12422-12429, 2001.

10. **Gimpl, G, Burger K, and Fahrenholz F.** Cholesterol as modulator of receptor function. *Biochemistry* 36: 10959-10974, 1997.

11. **Hill, WG, An B, and Johnson JP.** Endogenously Expressed Epithelial Sodium Channel Is Present in Lipid Rafts in A6 Cells. *J Biol Chem* 277: 33541–33544, 2002.

12. **Ikonen, E.** Roles of lipid rafts in membrane transport. *Curr Opin Cell Biol* 13: 470-477, 2001.

13. **Jans, D, De Weer P, Srinivas SP, Larivière E, Simaels J, and Van Driessche W.** Mg^{2+}-sensitive non-capacitative basolateral Ca^{2+} entry secondary to cell swelling in the polarized renal A6 epithelium. *J Physiol* 541: 91-101, 2002.

14. **Jans, D, Simaels J, Cucu D, Zeiske W, and Van Driessche W.** Effects of extracellular Mg^{2+} on transepithelial capacitance and Na$^+$ transport in A6 cells under different osmotic conditions. *Pflügers Arch – Eur J Physiol* 439: 504–512, 2000.

15. **Jans, D, Simaels J, Larivière E, Steels P, and Van Driessche W.** Extracellular Ca^{2+} regulates the stimulation of Na^+ transport in A6 renal epithelia. *Am J Physiol Renal Physiol* 287: F840-F849, 2004.

16. **Kato, N, Nakanishi M, and Hirashima N.** Cholesterol depletion inhibits store-operated calcium currents and exocytotic membrane fusion in RBL-2H3 cells. *Biochemistry* 42: 11808-11814, 2003.

17. **Lau, YT.** Cholesterol enrichment inhibits Na^+/K^+ pump in endothelial cells. *Atherosclerosis* 110: 251–257, 1994.

18. **Leonard, A, and Dufourc EJ.** Interactions of cholesterol with the membrane lipid matrix. A solid state NMR approach. *Biochimie* 73: 1295–1302, 1991.

19. **Lewis, SA, Eaton DC, Clausen C, and Diamond JM.** Nystatin as a probe for investigating the electrical properties of a tight epithelium. *J Gen Physiol* 70: 427-440, 1977.

20. **Lichtenstein, NS, and Leaf A.** Effect of amphotericin B on the permeability of the toad bladder. *J Clin Invest* 44: 1328-1342, 1965.

21. **Lijnen, P, and Petrov V.** Cholesterol modulation of transmembrane cation transport systems in human erythrocytes. *Biochem Mol Med* 56: 52-62, 1995.

22. **Ohtani, Y, Irie T, Uekama K, Fukunaga K, and Pitha J.** Differential effects of alpha-, beta- and gamma-cyclodextrins on human erythrocytes. *Eur J Biochem* 186: 17-22, 1989.

23. **Prince, LS, and Welsh MJ.** Effect of subunit composition and Liddle's syndrome mutations on biosynthesis of ENaC. *Am J Physiol Cell Physiol* 276: C1346–C1351, 1999.

24. **Rossier, BC, Canessa CM, Schild L, and Horisberger JD.** Epithelial sodium channels. *Curr Opin Nephrol Hypertens* 3: 487–496, 1994.

25. **Shlyonsky, VG, Mies F, and Sariban-Sohraby S.** Epithelial sodium channel activity in detergent-resistant membrane microdomains. *Am J Physiol Renal Physiol* 284: F182–F188, 2003.

26. **Simons, K, and Ikonen E.** How cells handle cholesterol. *Science* 290: 1721–1726, 2000.

27. **Simons, K, and Ikonen E.** Functional rafts in cell membranes. *Nature* 387: 569-572, 1997.

28. **Van Driessche, W, De Smet P, and Raskin G.** An automatic monitoring system for epithelial cell height. *Pflügers Arch* 425: 164-171, 1993.

29. **Van Driessche, W, De Vos R, Jans D, Simaels J, De Smet P, and Raskin G.** Transepithelial capacitance decrease reveals closure of lateral interspace in A6 epithelia. *Pflügers Arch* 437: 680–690, 1999.

30. **Van Driessche, W, and Lindemann B.** Low-noise amplification of voltage and current fluctuations arising in epithelia. *Rev Sci Instrum* 49: 53-57, 1978.

31. **Wang, H, Zajicek H, Kumar V, Wilson P, and Levi M.** Role of cholesterol in the regulation of renal phosphate transport. *Front Biosci* 2: d43-d48, 1997.

32. **Yeagle, PL, Young J, and Rice D.** Effects of cholesterol on Na^+,K^+-ATPase ATP hydrolyzing activity in bovine kidney. *Biochemistry* 27: 6449–6452, 1988.

[3]Laboratory of Biophysics,
International Centre of Biodynamics (ICB),
46-48 Calea Plevnei,
R-010233 BUCHAREST (Romania)

[4]Dept. of Health and Environmental Physics
Horia Hulubei National Institute for Physics and Nuclear Engineering
R-76900 BUCHAREST (Romania)

	NaCl	KHCO$_3$	CaCl$_2$	sucrose	MβCD
CTRL 260-I	135	2.5	1		
CTRL 140	50	2.5	1	35	
mβCD 140	50	2.5	1		20
CTRL 200-I	80	2.5	1	40	
mβCD 200-I	80	2.5	1		20
CTRL 200-II	102	2.5	1		
mβCD 200-II	102	2.5	1		10
CTRL 260-II	114	2.5	1	39	
MβCD 260	114	2.5	1		20

Table 1 – **Solution composition for electrophysiological recordings**
Concentrations are given in mM. Numbers in solution names indicate solution
osmolalities in mosmol/kg H$_2$O. The pH of the solutions was 8.2.

Stimulation type		Control			mβCD			N
		I_{SC} (μA/cm^2)	G_T (mS/cm^2)	C_T (μF/cm^2)	I_{SC} (μA/cm^2)	G_T (mS/cm^2)	C_T (μF/cm^2)	
S1	Basal	0.8 ± 0.1	0.07 ± 0.01	0.75 ± 0.01	1.1 ± 0.2	0.07 ± 0.01	0.81 ± 0.01	5
	Hyposhock	10.5 ± 0.9	0.14 ± 0.01	1.24 ± 0.06	6.9 ± 0.3	0.11 ± 0.01	1.40 ± 0.06	
	Δ Hypo – Basal	9.7 ± 0.8 [#]	0.07 ± 0.01 [*]	0.49 ± 0.03 [&]	5.8 ± 0.1 [#]	0.04 ± 0.01 [*]	0.59 ± 0.07 [&]	
S2	Basal	17.5 ± 1.7	0.20 ± 0.02	0.77 ± 0.03	15.7 ± 0.7	0.18 ± 0.01	0.74 ± 0.02	4
	Oxytocin	25.0 ± 1.9	0.36 ± 0.02	0.85 ± 0.04	19.7 ± 0.9	0.29 ± 0.01	0.81 ± 0.02	
	Δ Oxy - Basal	7.5 ± 0.5 [#]	0.16 ± 0.01 [*]	0.08 ± 0.01 [&]	4.0 ± 0.4 [#]	0.11 ± 0.01 [*]	0.07 ± 0.01 [&]	
S3	Basal	11.2 ± 0.6	0.15 ± 0.01	0.70 ± 0.01	12.9 ± 0.4	0.17 ± 0.01	0.73 ± 0.01	5
	Adenosine	20.2 ± 0.2	0.23 ± 0.01	0.77 ± 0.01	17.6 ± 0.7	0.21 ± 0.01	0.80 ± 0.01	
	Δ Adeno – Basal	9.0 ± 0.7 [#]	0.08 ± 0.01 [*]	0.07 ± 0.01 [&]	4.7 ± 0.7 [#]	0.04 ± 0.01 [*]	0.07 ± 0.01 [&]	

Table 2 - I_{SC}, G_T and C_T responses for control and apically cholesterol depleted cells during different Na$^+$ transport stimulations

Cells were treated with 20 mM mβCD (S1, S2) and 10 mM mβCD (S3), respectively. For mβCD treated cells the basal values considered are those obtained after 60 min of treatment (see text). For stimulated conditions I_{SC}, G_T and C_T were recorded at the time of maximal increase. Means $\pm$ S.E.M. for N tissues were calculated from experiments following the protocols presented in the results section. [#] [*] $P<0.05$ and [&] $P>0.05$ for comparison between corresponding electrical parameters variation for control and cholesterol depleted cells in each type of stimulation.
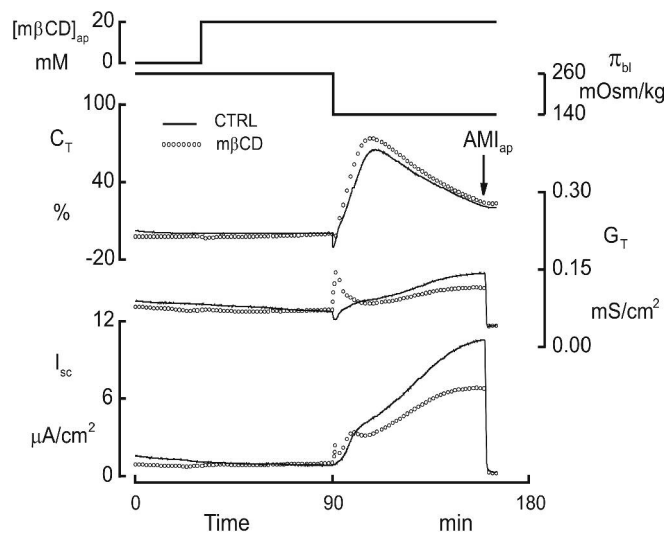
Figure 1 - Effect of mβCD on the response to hypotonicity
Time courses for I_{SC}, G_T, C_T in basal steady state conditions and in response to hypotonic shock in control (solid lines) and tissues treated for the indicated period with 20 mM mβCD on the apical side (dotted lines). The traces are mean values from 5 tissues in each case. The means $\pm$ SEM were omitted in the graphs for clarity.
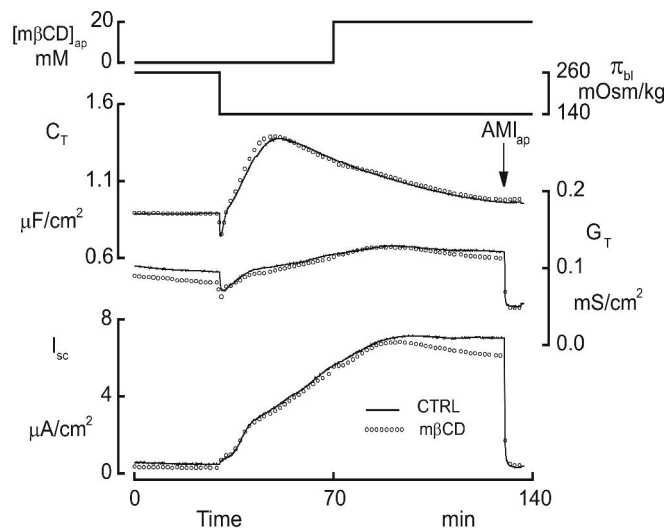

Figure 2 - Effect of apical treatment with 20 mM mβCD applied in highly stimulated conditions of hyposhock

Solid lines: control; dotted lines: apically cholesterol depleted cells. Traces represent the mean of 5 experiments.
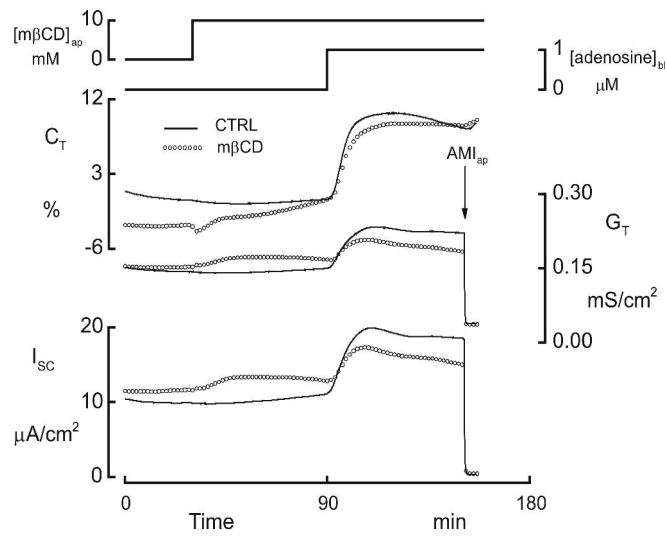
Figure 3 - Effects of cholesterol depletion on the activation of Na$^+$ transport by adenosine

Time courses of I_{SC}, G_T, C_T at 200 mOsm/kgH$_2$ in basal steady state conditions and in response to basolateral adenosine. Control experiments (solid lines) are compared with experiments in the presence of 10 mM mβCD (dotted lines) used to extract cholesterol from the apical side (N=5).
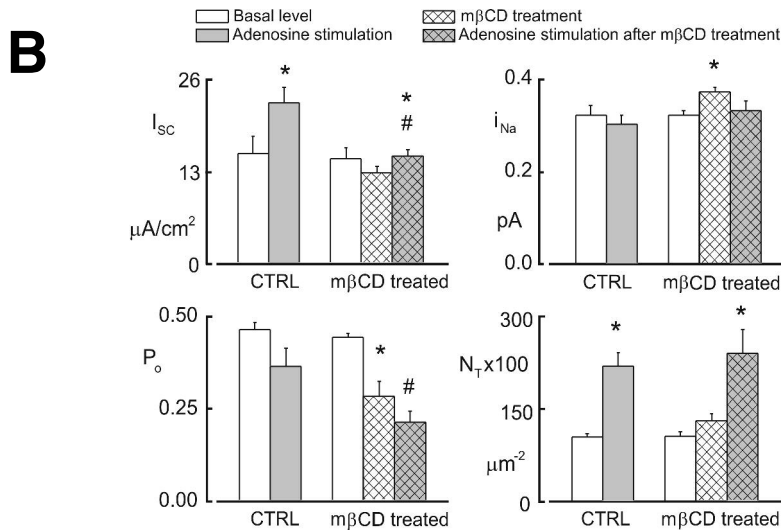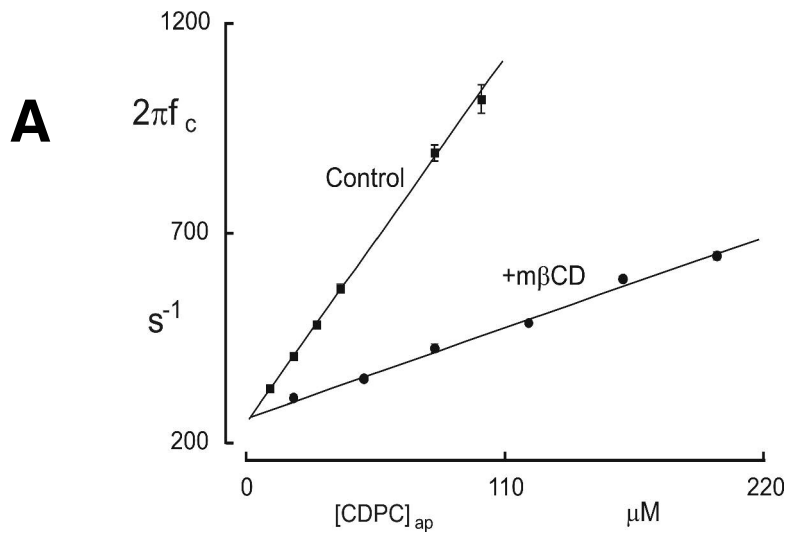
Figure 4 - Noise analysis parameters

A. Relationship between $2\pi f_c$ and the CDPC concentration in the absence (Control) and in the presence of 10 mM mβCD in the apical solution. The slope and intercept of the linear regressions for the control and in the presence of mβCD indicate the *ON* and *OFF* rates of the interaction between CDPC and the Na^+ channel in each case, respectively.

B. Results of noise analysis calculations represented in bar diagrams. I_{SC}, i_{Na}, N_T and P_o values in control (basal level and response to adenosine stimulation) are compared to the corresponding values obtained after apically treating the cells 1h with 10 mM mβCD. *$P < 0.05$ for comparison of the parameters inside each type of experiment. # $P<0.05$ for comparison between control and cholesterol depleted cells.
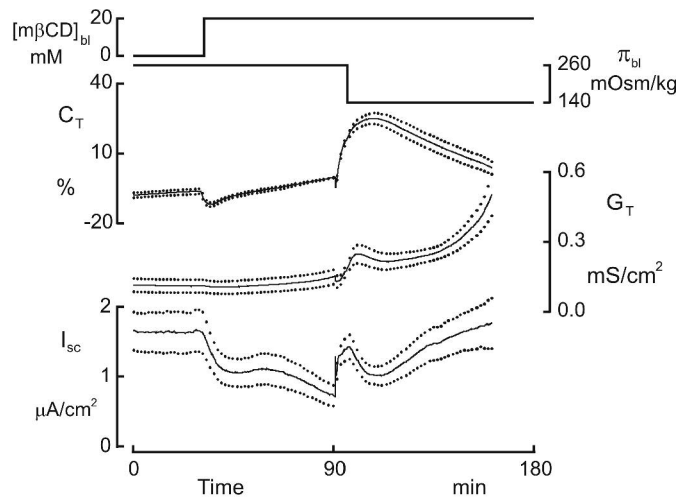
Figure 5 - Effect of basolateral cholesterol depletion on Na$^+$ transport
Time courses for I_{SC}, G_T and C_T in basal steady state conditions and in response to hypotonic shock after cholesterol depletion on basolateral side. Solid lines represent averaged values for a set of 4 experiments, whereas dashed lines depict the ± SEM values.
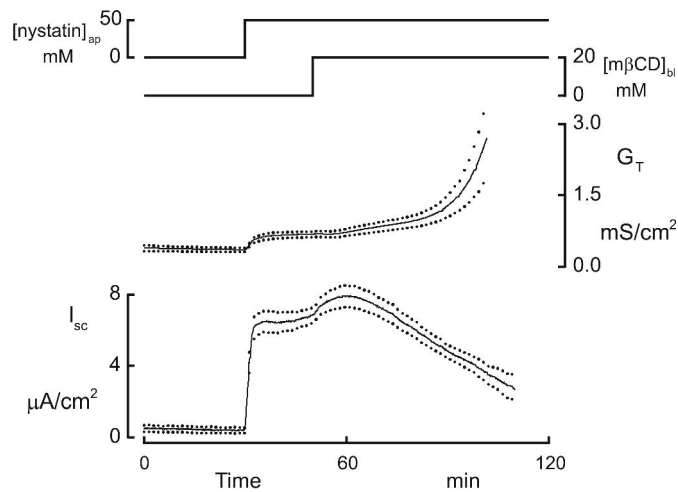

Figure 6 - Permeabilization of the apical membrane with nystatin

Averaged time courses (solid lines) and ± SEM traced (dashed lines) for I_{SC} and G_T in response to apical nystatin addition and subsequent basolateral treatment with 20 mM mβCD (N=4).